Supporting Information

Naturally Occurring Pentacyclic Triterpenes as Inhibitors of Glycogen Phosphorylase: Synthesis, Structure-Activity Relationships and X-ray Crystallographic Studies

Xiaoan Wen, Hongbin Sun, Jun Liu, Keguang Cheng, Pu Zhang, Liying Zhang, Jia Hao, Luyong Zhang, Peizhou Ni, Spyros E. Zographos, Demetres D. Leonidas, Kyra-Melinda Alexacou, Joseph M. Hayes, Thanasis Gimisis, Nikos G. Oikonomakos

Table of content:

Table S1 [a]

Compd.	IR	MS (m/z)	^{1}HNMR	^{13}CNMR	HRMS	
					Calcd.	Found
2	√	479 [M+Na]	√			
3	√	471 [M-H]	√	√	$C_{30}H_{47}O_4$ [M-H]: 471.3474	471.3465
4	√	473 [M+H]	√	√	$C_{30}H_{47}O_4$[M-H]: 471.3474	471.3495
5	√	495 [M+Na]	√	√	$C_{30}H_{47}O_4$ [M-H]: 471.3474	471.3470
6	√	453 [M-H]	√			
11	√	479 [M+Na]	√			
12	√	495 [M+Na]	√	√	$C_{30}H_{47}O_4$[M-H] : 471.3474	471.3453
13	√	495 [M+Na]	√	√	$C_{30}H_{47}O_4$ [M-H]: 471.3474	471.3485
14	√	495 [M+Na]	√	√	$C_{30}H_{47}O_4$ [M-H]: 471.3474	471.3481
17	√	477 [M+Na]	√			
18	√	641 [M+Na]	√	√		
19	√	641 [M+Na]	√	√		
20	√	657 [M+Na]	√	√		
26	√	569 [M+Na]	√			
27	√	547[M+H]	√			
28	√	567 [M+Na]	√		$C_{37}H_{51}O_3$ [M-H]: 543.3838	543.3865
29	√	567 [M+Na]	√		$C_{37}H_{51}O_3$ [M-H]:543.3838	543.3851
32	√	585 [M+Na]	√		$C_{37}H_{53}O_4$[M-H]: 561.3944	561.3929
33	√	585 [M+Na]	√	√	$C_{37}H_{53}O_4$ [M-H]: 561.3944	561.3969
34			√	√	$C_{37}H_{51}O_4$ [M-H]: 559.3787	559.3815
35	√	561 [M+H]	√	√	$C_{37}H_{51}O_4$ [M-H]: 559.3787	559.3811
36	√	585 [M+Na]	√	√	$C_{37}H_{53}O_4$ [M-H]: 561.3944	561.3962
37	√	585 [M+Na]	√	√	$C_{37}H_{53}O_4$ [M-H]: 561.3944	561.3964
38	√	559 [M+H]	√	√	$C_{37}H_{49}O_4$ [M-H]: 557.3631	557.3657
39	√	559 [M+H]	√	√	$C_{37}H_{49}O_4$[M-H]: 557.3631	557.3651
40	√	585 [M+Na]	√	√	$C_{37}H_{53}O_4$ [M-H]: 561.3944	561.3971
41	√	585 [M+Na]	√	√	$C_{37}H_{53}O_4$ [M-H]: 561.3944	561.3959
42	√	561 [M+H]	√	√	$C_{37}H_{51}O_4$ [M-H]: 559.3787	557.3808
43	√	569 [M+Na]	√			
44	√	569 [M+Na]	√			
46	√	809 [M+Na]	√	√		

47	√	809 [M+Na]	√	√		
48	√	825 [M+Na]	√	√		

[a] The target compounds **2-6**, **11-14** and **17-20** are all known naturally occurring products, and their analytical data was identical with the reported data (see experimental). Typically, purities were >98%.

Table S2

Summary of diffraction data and refinement statistics for the GPb-Asiatic Acid complex	
Experiment	10 mM Asiatic Acid (7 h)
Space group	$P4_32_12$
No. of images (°)	80 (0.8)[1]
Unit cell dimensions (Å)	a=b=128.72, c=116.64
Resolution range (Å)	30 – 2.4
No. of observations	779188
No. of unique reflections	38832
$\langle I/\sigma(I)\rangle$ (outermost shell)[2]	15.5 (4.2)
Completeness (outermost shell) (%)	100 (99.9)
R_m (outermost shell)[3]	0.070 (0.471)
Outermost shell (Å)	2.44-2.40
Redundancy (outermost shell)	5.3 (5.4)
Refinement (resolution) (Å)	90.91 – 2.40
No of reflections used (free)	36836 (1942)
Residues included	(12-254), (261-317), (324-836)
No of protein atoms	6623
No of water molecules	198
No of ligand atoms	15 (PLP), 35 (Asiatic acid)
R (outermost shell) (%)	17.9 (22.6)
(R_{free})[4] (outermost shell) (%)	20.8 (30.7)
Outermost shell in refinement (Å)	2.46-2.40
r.m.s.d. in bond lengths (Å)	0.008
r.m.s.d. in bond angles (°)	1.13
Average *B* (Å^2) for residues	(12-254), (261-317), (324-836)
Overall	40.1
Main chain	39.4
Side chain	40.8
Average *B* (Å^2) for ligands	27.8 (PLP), 80.7 (Asiatic acid)
Average *B* (Å^2) for Water molecules	38.5

[1] 0.8 is the rotation range per image

[2] $\sigma(I)$ is the standard deviation of *I*.

[3]$R_{merge} = \Sigma_i \Sigma_h | \langle I_h \rangle - I_{ih} | / \Sigma_i \Sigma_h I_{ih}$, where $\langle I_h \rangle$ and I_{ih} are the mean and ith measurement of intensity for reflection h, respectively.

[4]Crystallographic $R = \Sigma | |\boldsymbol{F}_o| - |\boldsymbol{F}_c| | / \Sigma |\boldsymbol{F}_o|$, where $|\boldsymbol{F}_o|$ and $|\boldsymbol{F}_c|$ are the observed and calculated structure factor amplitudes, respectively. R_{free} is the corresponding R value for a randomly chosen 5% of the reflections that were not included in the refinement.

Table S3

Summary of diffraction data and refinement statistics for the GPb-Maslinic Acid complex	
Experiment	10 mM Maslinic Acid (7 h)
Space group	$P4_32_12$
No. of images (°)	80 (0.8)[1]
Unit cell dimensions (Å)	a=b=128.72, c=116.70
Resolution range (Å)	30 – 2.7
No. of observations	795136
No. of unique reflections	27542
<I/σ(I)> (outermost shell)[2]	17.2 (4.2)
Completeness (outermost shell) (%)	99.8 (99.7)
R_m (outermost shell)[3]	0.077 (0.492)
Outermost shell (Å)	2.75-2.70
Redundancy (outermost shell)	5.3 (5.4)
Refinement (resolution) (Å)	90.91 – 2.70
No of reflections used (free)	26130 (1383)
Residues included	(12-254), (261-317), (324-836)
No of protein atoms	6623
No of water molecules	129
No of ligand atoms	15 (PLP), 34 (Maslinic acid)
R (outermost shell) (%)	16.7 (23.7)
(R_{free})[4] (outermost shell) (%)	22.3 (31.1)
Outermost shell in refinement (Å)	2.77-2.70
r.m.s.d. in bond lengths (Å)	0.009
r.m.s.d. in bond angles (°)	1.18
Average *B* (Å^2) for residues	(12-254), (261-317), (324-836)
Overall	42.2
Main chain	41.6
Side chain	42.9
Average *B* (Å^2) for ligands	29.8 (PLP), 82.7 (Maslinic acid)
Average *B* (Å^2) for Water molecules	36.5

[1] 0.8 is the rotation range per image

[2] $\sigma(I)$ is the standard deviation of I.

[3] $R_{merge} = \Sigma_i \Sigma_h | \langle I_h \rangle - I_{ih} | / \Sigma_i \Sigma_h I_{ih}$, where $\langle I_h \rangle$ and I_{ih} are the mean and ith measurement of intensity for reflection h, respectively.

[4] Crystallographic $R = \Sigma | |\boldsymbol{F}_o| - |\boldsymbol{F}_c| | / \Sigma |\boldsymbol{F}_o|$, where $|\boldsymbol{F}_o|$ and $|\boldsymbol{F}_c|$ are the observed and calculated structure factor amplitudes, respectively. R_{free} is the corresponding R value for a randomly chosen 5% of the reflections that were not included in the refinement.

Table S4

Hydrogen bond interactions between Asiatic acid and GPb residues at the allosteric site

Inhibitor atom	Protein atom	Distance (Å)
O3	Gln72 NE2	2.8
	Asp42′ OD2	2.7
O29	Arg310 NE	3.2
	Arg310 NH1	2.7
O28	Arg310 NE	2.8
O23	Asp42′ OD1	2.9

Table S5

Hydrogen bond interactions between Maslinic acid and GPb residues at the allosteric site

Inhibitor atom	Protein atom	Distance (Å)
O3	Gln72 NE2	2.8
	Asp42′ OD2	2.7
O29	Arg310 NH1	2.7
O28	Arg310 NE	2.8

Table S6

Van der Waals interactions between Asiatic acid and GPb residues at the allosteric site

Inhibitor atom	Protein atom	No of contacts
O3	Gln72 CD,OE1; Asp42′ CG,OD1; Asn44′ ND2	5
C3	Gln72 NE2; Asp42′ OD1,OD2	3
C2	Gln72 CD,OE1,NE2	3
O2	Gln72 OE1	1
C1	Val45′ CG1	1
C25	Gln71 O,C; Tyr75 CB	3
C11	Tyr75 CD1	1
C21	Arg309 CZ,NH2	2
C22	Arg309 NH2	1
C28	Arg310 NE,NH1,CZ	3
O29	Arg310 CZ	1
O28	Arg310 NH1,CG,CD,CZ; Wat102	5
C26	Wat102	1
C16	Phe196 CZ	1
C5	Val45′ CG1	1
C24	Ile68 CG2,O; Gln72 N,CA,CB,NE2	6
C23	Ile68 CG2; Asp42′ CG,OD1,OD2	4
O23	Asp42′ N,CG,OD2; Val45′CB,CG1,CG2	6
Total		**48**

Table S7

Van der Waals interactions between Maslinic acid and GPb residues at the allosteric site

Inhibitor atom	Protein atom	No of contacts
O3	Gln72 CD,OE1; Asp42′ CG,OD1; Asn44′ ND2	5
C3	Gln72 NE2; Asp42′ OD1,OD2	3
C2	Gln72 OE1	1
O2	Gln72 OE1	1
C1	Val45′ CG1	1
C25	Gln71 O,C	2
C21	Arg309 CZ,NH1,NH2	3
C22	Arg309 NH2	1
C28	Arg310 NE,NH1,CZ	3
O29	Arg242 CZ,NH1,NH2; Arg310 NE,CZ	5
O28	Arg310 NH1,CG,CD,CZ	3
C16	Phe196 CE1,CZ,CE2	3
C5	Val45′ CG1	1
C24	Ile68 O; Gln72 N,NE2	3
C23	Asp42′ CG,OD1,OD2; Val45′ CG2	4
C29	Arg309 CG	1
Total		**40**

Figure S1

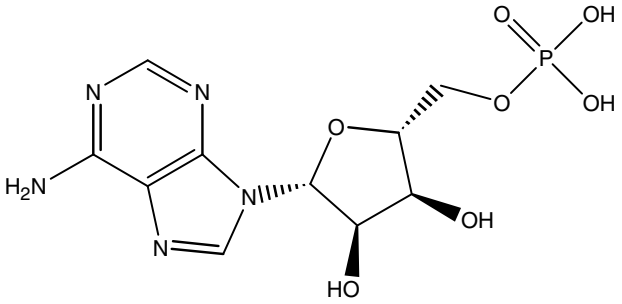

AMP

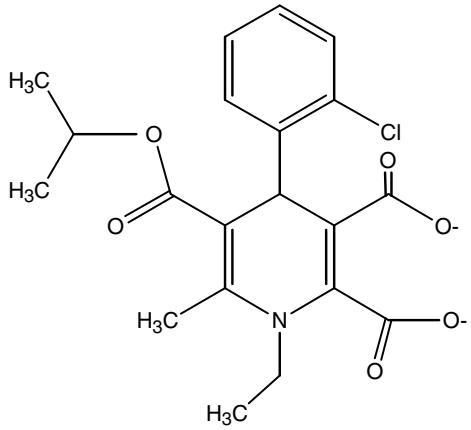

W1807

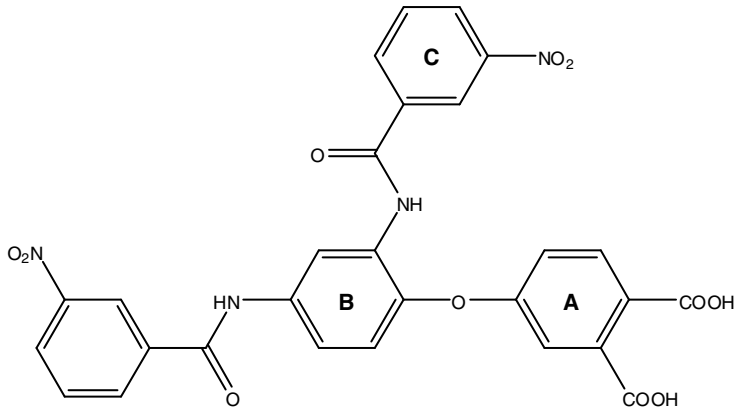

Novo4j

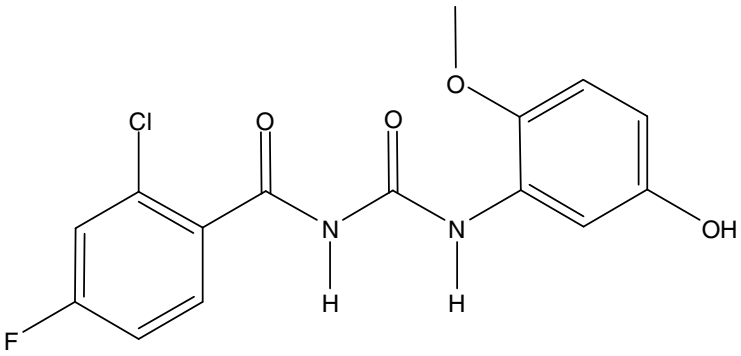

AVE#21

Comparison with 1-(2-chloro-4-fluorobenzoyl)-3-(5-hydroxy-2-methoxy-phenyl) urea (Bayer compound W1807).

Bayer compound W1807 is the most potent inhibitor of rabbit muscle GP known to date (K_i =1.6 nM for GPb and K_i =10.8 nM for GPa). Superposition of the complex structures of GPb-**15** and GPb-W1807 (Figure S2) reveals that W1807 partially overlaps with **15**. The 1,4-hidydro-1-ethyl-2-methyl-3-caboxylate-pyridine ring superimposes onto **B** and **C** rings; the two carboxylates of W1807 exploit the allosteric effector phosphate recognition site and are close to the carboxylate oxygens O23 and O24 of **15**; the chlorophenyl group of W1807 is oriented almost perpendicular to the **C** ring. Compound **15** makes hydrogen bonding interactions with one arginine (Arg310), and a few nonpolar van der Waals interactions to Tyr75, Phe196, and Val45'. In contrast, the contacts from W1807 to GPb are dominated by nonpolar van der Waals interactions (to Val45', Trp67, Ile68, Tyr75 and interactions from the (δ^- π) electron cloud of the chlrorophenyl ring to the (δ^+) hydrogen atoms on the Phe196) and also by ionic interactions from the carboxylate groups to three arginine residues (Arg242, Arg309, and Arg310). This may explain why W1807 is a much more potent inhibitor than **15**.

Figure S2 Comparison between GPb-asiatic acid complex (shown in green-subunit 1 and orange-subunit 2) and T-state GPb-W1807 (shown in mauve-subunit 1 and cyan-subunit 2).

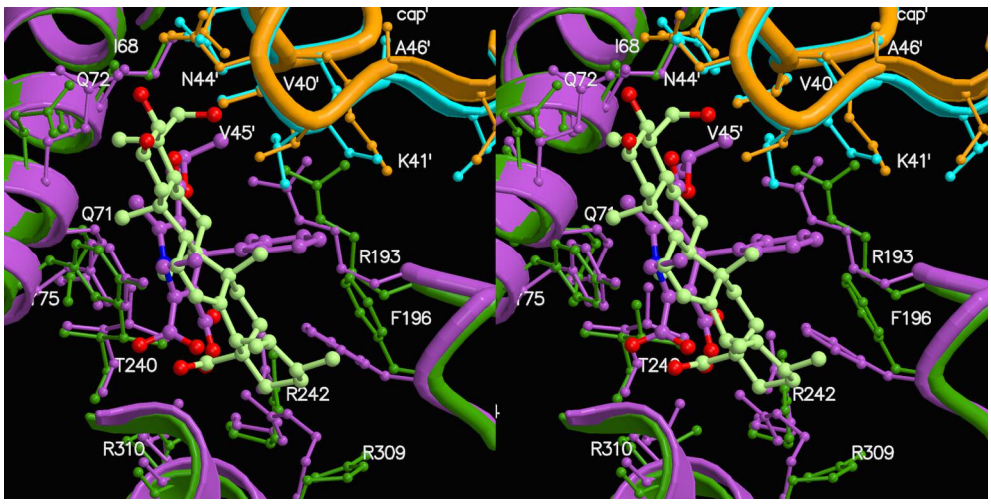

Comparison with 4-[2,4-bis-(3-nitrobenzoylamino)phenoxy]phthalic acid (Novo4j)

4-[2,4-Bis-(3-nitrobenzoylamino)phenoxy]phthalic acid (**Novo4j**) was found to be a potent inhibitor of pig liver GPa (with an IC_{50} value of 74 nM) that also binds at the allosteric site of the rabbit muscle enzyme. Compound **Novo4j,** on binding to GPb, induces conformational changes to the enzyme and stabilises a conformation similar to that of GPb-**15**. The structural comparison of GPb-**Novo4j** and GPb-**15** complexes shows (Figure S3) that rings **A** and **B** of **Novo4j** overlap with rings **A-D** and the carboxylate of **15**, while the two 3-nitrobenzoylamino groups of **Novo4j** fit the space available in the allosteric site are directed towards the narrow side pocket of the AMP site (between Trp67 and Arg193) and to the entrance of the AMP site (Asp42', Gln44' and Gln72), respectively, and do not overlap with **15**.

Figure S3. Comparison between GPb-asiatic acid complex (shown in green-subunit 1 and orange-subunit 2) and T-state GPb-novo4j (shown in mauve-subunit 1 and cyan-subunit 2).

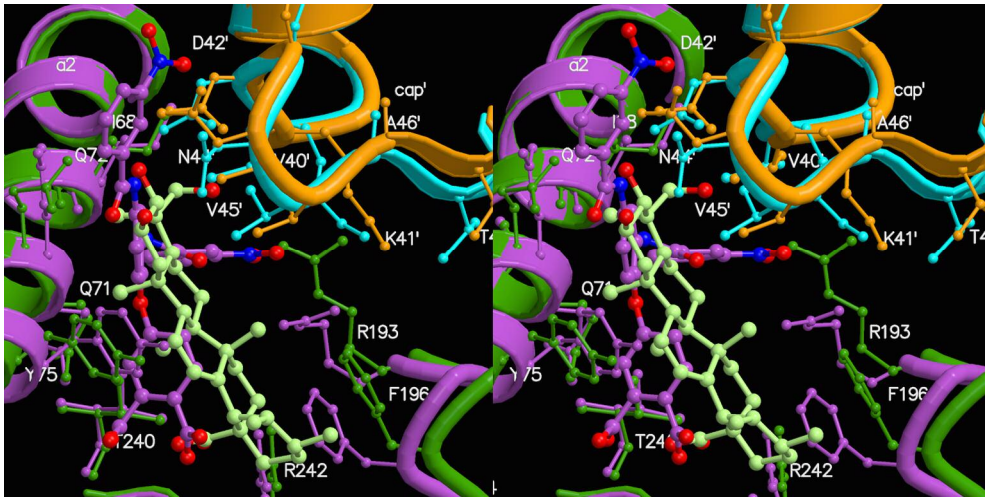

Comparison with 1-(2-chloro-4-fluorobenzoyl)-3-(5-hydroxy-2-methoxy-phenyl) urea (AVE#21)

Compound **AVE#21**, with an enzymic activity of IC_{50}=23 (±1) nM, is one of the most potent inhibitors of human liver glycogen phosphorylase (hlGPa) that binds at the allosteric site. The compound binds with 2-chloro-4-fluoro-substituted benzoyl ring buried deep in the allosteric site and tightly packs against Trp67, Arg193, Val40', and Lys41'; the central acyl urea moiety makes hydrogen bonding interactions with the carbonyl group of Val40', the backbone amide group of Asp42', and an ordered water molecule in the upper part of the AMP pocket; the phenolic ring, which points toward the entrance of the site, makes hydrogen bonds with Asp42' and Asn44' and makes additional van der Waals interactions with Tyr75 through the methoxy substituent. These interactions may provide an explanation for the high potency of **AVE#21**. The superposition of the structure of the hlGPa-**AVE#21** complex with GPb-**15** complex shows (Figure S4). The 5-hydroxy-2-methoxy-phenyl ring overlaps mostly with **A** ring and only partially with **B** ring of compound **15**, while the 2-chloro-4-fluoro-substituted benzoyl ring of **AVE#21** do not overlap with **15**.

Figure S4. Comparison between GPb-asiatic acid complex (shown in green-subunit 1 and orange-subunit 2) and T-state hlGPa-AVE#21 (shown in mauve-subunit 1 and cyan-subunit 2).

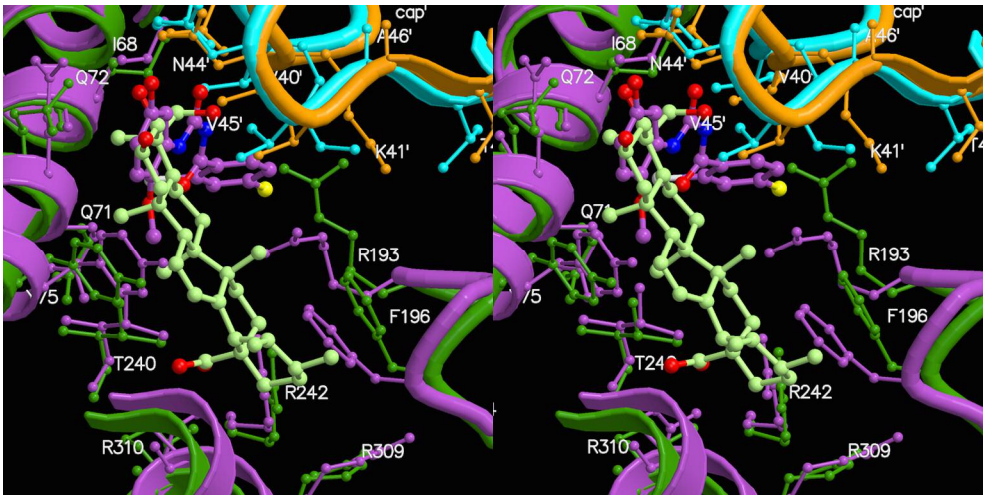

Figure S5. Comparison of the position of the asiatic acid as compared to those of AMP (a), W1807 (b), **novo4j** (c), and **AVE#21** (d), after superimposing the corresponding complex structures onto the GPb-asiatic acid complex structure.

(a)

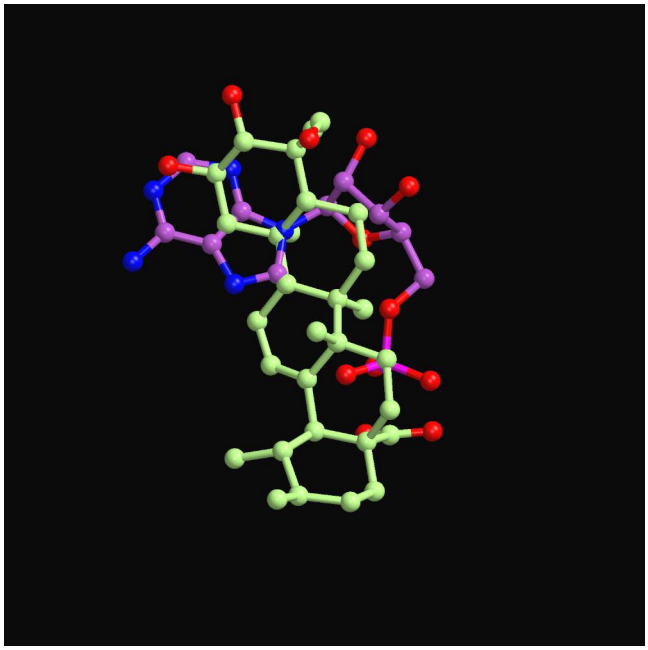

(b)

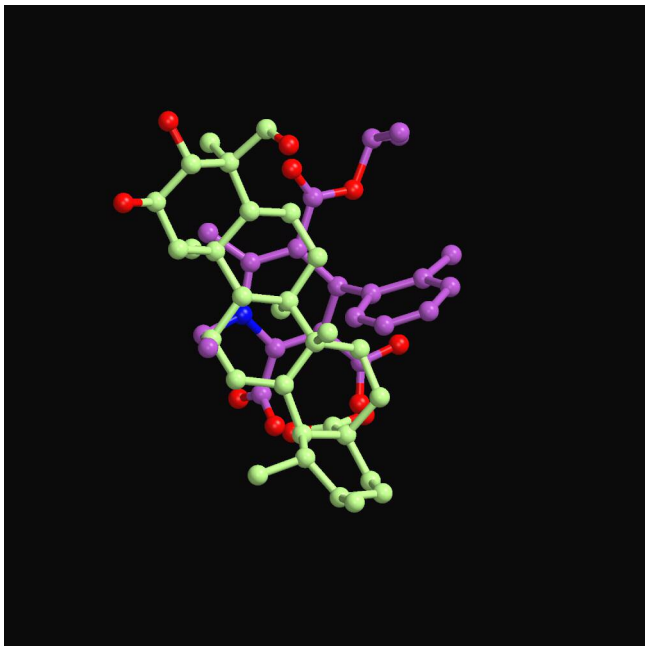

(c)

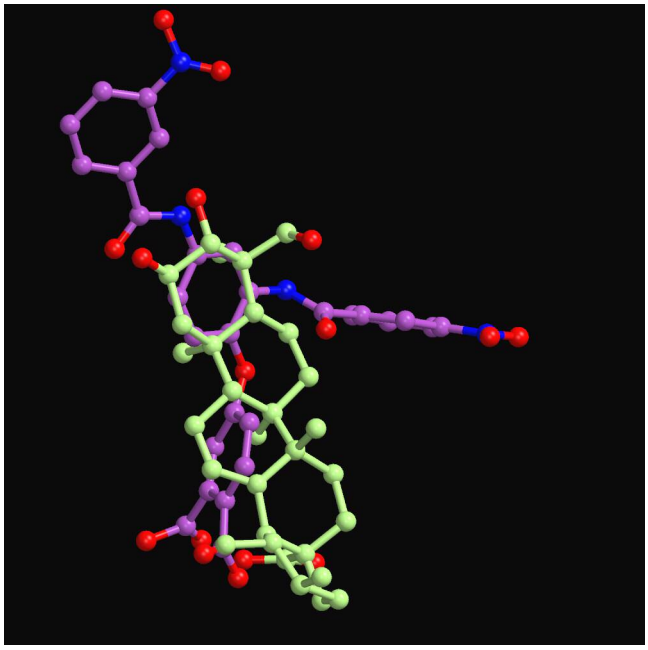

(d)